Vol 16 No 8, August 2007
1009-1963/2007/16(08)/2244-10

Chinese Physics

© 2007 Chin. Phys. Soc.
and IOP Publishing Ltd

Generation and control of chaos in a Bose–Einstein condensate*

Xu Jun(徐 军), Hai Wen-Hua(海文华)†, and Li Hui(李 辉)

Department of Physics, Hunan Normal University, Changsha 410081, *China*

(Received 1 January 2007; revised manuscript received 10 January 2007)

For a Bose–Einstein condensate (BEC) confined in a double lattice consisting of two weak laser standing waves we find the Melnikov chaotic solution and chaotic region of parameter space by using the direct perturbation method. In the chaotic region, spatial evolutions of the chaotic solution and the corresponding distribution of particle number density are bounded but unpredictable between their superior and inferior limits. It is illustrated that when the relation $k_1 \approx k_2$ between the two laser wave vectors is kept, the adjustment from $k_2 < k_1$ to $k_2 \geq k_1$ can transform the chaotic region into regular one or the other way round. This suggests a feasible scheme for generating and controlling chaos, which could lead to an experimental observation in the near future.

Keywords: Bose–Einstein condensate, double lattice, chaotic region, control
PACC: 0530J, 0545, 3690

1. Introduction

The creation of Bose–Einstein condensate (BEC) and the corresponding macroscopic quantum phenomenon have attracted much attention and provided a platform for investigating many important phenomena in atomic physics, condensed-matter physics, quantum computation and quantum information.[1,2] Correlated physical properties including superfluidity,[3,4] macroscopic quantum self-trapping,[5,6] soliton and chaos[7−11] have been investigated extensively. Under the mean-field theory, the BEC is described by the Gross–Pitaevskii equation (GPE), which is a nonlinear Schrödinger equation with the nonlinear term representing interaction between the condensed atoms. Because of the nonlinearity, there exists the interesting chaos phenomenon in the system. Recently, chaotic behaviours in BEC have widely received much attention; one is interested in the chaos in collapsing BEC,[12,13] chaotic self-trapping,[14] classical[15] and quantum chaos,[16] chaos and energy exchange,[17] coherent atomic oscillations and nonlinear resonances of BEC,[18] and so on. In the previous work, we have investigated the time-dependent chaos of a BEC in moving optical lattice,[10] chaos and quantum entanglement,[19] chaotic probability density and frequency-locked atomic population oscillations.[20] We also discussed the chaotic features in the spatial evolution of stationary state BECs, which are trapped in a weak or strong optical lattice potential.[11] On account of chaos affecting the stability and collapsibility of BEC, one is desirous of controlling the chaos in BEC for the purpose of application.

Control of chaos has been one of the most hot subjects since Ott, Grebogi and Yorke proposed the well-known OGY feedback control of chaos.[21] On the basis of OGY method, one tries to control chaos in all kinds of ways and also has developed some new methods. These control methods can be separated into two categories: feedback (active) control and nonfeedback (passive) control. The feedback control may be further classified into the time-delayed feedback control,[22,23] spatial feedback control[24] and spatiotemporal feedback control.[25,26] Nonfeedback control contains resonant parametric perturbation control and weak parametric perturbations control.[27] Very interesting research has been carried out by using two adscititious lattice potentials.[28] Cohen and coworkers[29] discussed the quasiperiodic Fresnel atom optics and focusing, Chacón *et al*[27,30] used two time-dependent periodic potentials to suppress chaos, and Diener *et al*[31] investigated the transitions between extended and localized states in a one-dimensional incommensurate optical lattice, and so on.

*Project supported by the National Natural Science Foundation of China (Grant No 10575034), and the Key Laboratory of Magnetic Resonance and Atomic and Molecular Physics of China (Grant No T152504).
†Corresponding author. E-mail: adcve@public.cs.hn.cn

In this paper, we investigate a stationary BEC held in two weak laser standing waves whose GPE is similar to the temporal equation with two weak time-dependent periodic potentials.[27,30] Treating the two weak laser terms as the perturbation and using the direct perturbation expansion of the wavefunction to the first order approximation, the chaotic solution is obtained under the Melnikov chaos criterion. The chaotic orbit in equivalent phase space, spatial evolution images of the first perturbed solution and particle number density are plotted. Through the Melnikov function technique, the chaotic region of parameter space is found, which is correlated with the laser wave vectors. It is shown analytically and numerically that one can transform BEC from an aperiodic chaotic distribution into a periodic regular structure or the other way round by modulating the laser wave vectors, consequently, the chaos is generated or suppressed.

2. Melnikov chaotic solution and chaotic region in parameter space

We consider a BEC trapped in a periodic or quasi-periodic potential consisting of two 1-D weak laser standing waves. The GPE governing the system reads

$$\begin{aligned} \mathrm{i}h\frac{\partial\psi}{\partial t} &= -\frac{\hbar^2}{2m}\psi_{xx} + g_{1\mathrm{d}}|\psi|^2\psi \\ &\quad +(V_1\sin^2 k_1x - V_2\sin^2 k_2x)\psi, \end{aligned} \tag{1}$$

where m is the atomic mass, $g_{1\mathrm{d}}$ is the interaction intensity between the condensed atoms, V_1 and V_2 denote the strengthes of two laser standing waves, k_1 and k_2 are the laser wave vectors. Without loss of generality, we let the weak laser obey the relation $0 < V_1$, and $V_2 \ll E_r$, with $E_{\mathrm{r}} = \dfrac{\hbar^2k_1^2}{2m}$ being the recoil energy. The corresponding stationary state GPE can be written as

$$\begin{aligned} &-\frac{1}{2}\psi_{xx} + g|\psi|^2\psi + \left(V_1\sin^2 x - V_2\sin^2\frac{k_2}{k_1}x\right)\psi \\ &= \mu\psi. \end{aligned} \tag{2}$$

Here spatial coordinate x and macroscopic wavefunction ψ have been normalized in units of k_1^{-1} and $\sqrt{k_1}$, respectively, and laser intensities V_1, V_2 and chemical potential μ are normalized by two times the recoil energy, i.e. $2E_{\mathrm{r}}$ such that all variables and parameters in Eq.(2) are dimensionless. Consequently, the interatomic pseudopotential strength becomes $g = 4\pi a_s k_1$ with s-wave scattering length a_{s}. Writing wavefunction ψ in the form of $\psi = R(x)\exp[\mathrm{i}\theta(x)]$ and inserting it into Eq.(2), we obtain a couple of equations,

$$\begin{aligned} R_{xx} &= R\theta_x^2 + 2gR^3 \\ &\quad +2\left(V_1\sin^2 x - V_2\sin^2\frac{k_2}{k_1}x - \mu\right)R, \end{aligned} \tag{3}$$

$$\theta_{xx} + 2\theta_x R_x/R = 0, \tag{4}$$

with amplitude $R(x)$ and phase $\theta(x)$. Integrating Eq.(4) yields the flow speed in terms of the particle number density R^2,

$$v(x) = \hbar k_1\theta_x/m = c_1\hbar k_1/(mR^2), \tag{5}$$

where $c_1 = \theta_x(x_0)R^2(x_0)$ is an integration constant, which is determined by the flow speed and number density at boundary point x_0. Applying expression (5) to Eq.(3), yields

$$\begin{aligned} R_{xx} &= \frac{c_1^2}{R^3} + 2gR^3 \\ &\quad +2\left(V_1\sin^2 x - V_2\sin^2\frac{k_2}{k_1}x - \mu\right)R. \end{aligned} \tag{6}$$

Obviously, in the zero speed case, $c_1 = 0$, Eq.(6) is reduced to the parametrically driven Duffing equation for the spatial evolution. Generally, $c_1 \neq 0$, the system is quite complicated and difficult to solve analytically so that we have to seek its perturbed or numerical solutions. Choose the boundary speed $v(x_0) = 5.35\times10^{-3}$m/s for the ^{87}Rb atomic BEC and insert it into Eq.(5), then we will obtain the constants $\theta_x(x_0) = 1$ and $c_1 = \theta_x(x_0)R^2(x_0) = 0.01$. Choosing the equilibrium density amplitude and its derivative as $R_0(x_0) = 0.1$, and $R_{0,x}(x_0) = 0$ and taking the experiment parameters as $g = 0.5$, $\mu = 0.410278$, $k_1 = 0.48\times(2\pi/850)(\mathrm{nm})^{-1}$, $k_2 = 0.52\times(2\pi/850)(\mathrm{nm})^{-1}$, $V_1 = 0.0116698$, and $V_2 = 0.02$, we have the orbit in the equivalent phase space $(R(x),\ \mathrm{d}R(x)\mathrm{d}x)$ as in Fig.1. Therefore, we expect the existence of chaotic solution for this nonlinear system, because of the confuse structure in a finite phase region.

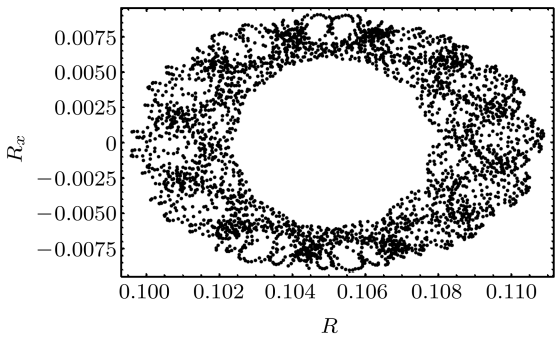


Fig.1. The chaotic orbit in equivalent phase space (R, R_x). The phase orbit is localized in a finite region and shows a confused structure. Here R and R_x are dimensionless.

Because it is difficult to find the exact solution of Eq.(6), we consider the two weak laser standing waves as a perturbation to seek the approximate chaotic solution. By using the direct perturbation method, we make a perturbation expansion of amplitude $R(x)$ to the first approximation, i.e. $R(x) = R_0(x) + R_1(x)$, and $\mid R_1(x) \mid \ll \mid R_0(x) \mid$. Inserting it into Eq.(6), we obtain the zeroth and first order equations as follows:

$$R_{0,xx} = \frac{c_1^2}{R_0^3} + 2gR_0^3 - 2\mu R_0, \tag{7}$$

$$\begin{aligned} R_{1,xx} &= -3c_1^2\frac{R_1}{{R^4}_0} + 6gR_0^2R_1 - 2\mu R_1 \\ &\quad +2\left(V_1\sin^2 x - V_2\sin^2\frac{k_2}{k_1}x\right)R_0. \end{aligned} \tag{8}$$

Integrating the zeroth equation leads to

$$\frac{1}{2}R_{0,x}^2 = -\frac{c_1^2}{2R_0^2} + \frac{1}{2}gR_0^4 - \mu R_0^2 + c_2, \tag{9}$$

with integration constant $c_2 = \frac{1}{2}R_{0,x}^2(x_0) + c_1^2/2R_0^2(x_0) - \frac{1}{2}gR_0^4(x_0) + \mu R_0^2(x_0)$, which is determined by the boundary conditions. We set the zeroth order density as $\rho_0(x) = R_0^2(x)$, so Eq.(9) becomes

$$\begin{aligned} \rho_{0,x}^2 &= 4g\rho_0^3 - 8\mu\rho_0^2 + 8c_2\rho_0 - 4c_1^2 \\ &= 4g(\rho_0 - a)(\rho_0 - b)(\rho_0 - c), \end{aligned} \tag{10}$$

with constants a, b, and c obeying

$$\begin{aligned} &a + b + c = \frac{2\mu}{g}, \\ &ab + bc + ca = \frac{2c_2}{g}, \quad \text{and} \quad abc = \frac{c_1^2}{g}. \end{aligned} \tag{11}$$

Letting the atom-atom interactions be repulsive with positive s-wave scattering length a_s and positive g through the Feshbach resonance and supposing $a \geq b > c$, the solution of Eq.(10) can be expressed as[11]

$$\begin{aligned} &\rho_0 = b - (b - c)cn^2(\zeta, K),\ \zeta = \sqrt{g(a - c)}(x - c_0), \\ &c_0 = x_0 \mp \frac{1}{\sqrt{g(a - c)}}F[\arcsin\sqrt{\frac{\rho_0(x_0) - c}{b - c}}, K], \quad \text{and} \quad K = \sqrt{\frac{b - c}{a - c}}, \end{aligned} \tag{12}$$

where $F[\phi, K] = \int_0^\phi \mathrm{d}\phi'(1 - K^2\sin^2\phi')^{-1/2}$ is the Legendre elliptic integral of the first kind with K being the modulus, and $\rho_0(x_0)$ is the equilibrium density at the boundary. Obviously, there are many different zeroth order solutions for different system parameters and equilibrium densities. If they satisfy the relation $(2\mu - \sqrt{16\mu^2 - 24gc_2})(4\mu + \sqrt{16\mu^2 - 24gc_2})^2 = 108g^2c_1^2$, and $a = b$, i.e. $K = 1$, solution (12) becomes the spatially homoclinic solution,[11]

$$\rho_0 = a - (a - c)\mathrm{sech}^2\zeta. \tag{13}$$

So the solution of Eq.(7) reads

$$R_0 = \sqrt{a - (a - c)\mathrm{sech}^2\zeta}, \tag{14}$$

which is sometimes referred to as a 'dark soliton' on a background of the BEC cloud.[32]

Inserting expression (14) into Eq.(8), we obtain the first approximation equation as a nonhomogeneous linear equation with variable coefficients. The corresponding homogeneous equation is given by Eq.(8) with $V_1 = V_2 = 0$. We use a useful method[11,33] to construct the general solution of Eq.(8). To start with, we construct two linear independent solutions of the homogeneous equation

$$\begin{aligned} R_1' &= \frac{\mathrm{d}R_0}{\mathrm{d}x} \\ &= \sqrt{g(a - c)}(a - c)\frac{\mathrm{sech}^2\zeta\tanh\zeta}{\sqrt{a - (a - c)\mathrm{sech}^2\zeta}}, \end{aligned} \tag{15}$$

$$R_1^{''} = R_1^{'}\int (R_1^{'})^{-2}\mathrm{d}x = \frac{1}{\sqrt{g(a-c)}}R_1^{'}\int (R_1^{'})^{-2}\mathrm{d}\zeta = \mathrm{sech}^2\zeta\tanh\zeta[12(a+4c)\zeta$$
$$-32c(\coth\zeta)+8(a+c)\sinh 2\zeta + a\sinh 4\zeta]/\left[32g(a-c)^2\sqrt{a-(a-c)\mathrm{sech}^2\zeta}\right]. \tag{16}$$

Obviously, $R_1^{'}$ is a bounded function of spatial coordinate, but $R_1^{''}$ includes a term proportional to function $\sinh 4\zeta$, which exponentially increases with the growth of ζ. Employing $R_1^{'}$ and $R_1^{''}$, the general solution of nonhomogeneous Eq.(8) can be written as

$$\begin{aligned} R_1 &= R_1^{''}\int_A^x R_1^{'}2\left(V_1\sin^2 x - V_2\sin^2\frac{k_2}{k_1}x\right)R_0\mathrm{d}x - R_1^{'}\int_B^x R_1^{''}2\left(V_1\sin^2 x - V_2\sin^2\frac{k_2}{k_1}x\right)R_0\mathrm{d}x \\ &= \frac{2}{\sqrt{g(a-c)}}\left[R_1^{''}(\zeta)\int_A^\zeta R_1^{'}(\zeta)V(\zeta)R_0(\zeta)\mathrm{d}\zeta - R_1^{'}(\zeta)\int_B^\zeta R_1^{''}(\zeta)V(\zeta)R_0(\zeta)\mathrm{d}\zeta\right], \\ V(\zeta) &= V_1\sin^2\left[\zeta/\sqrt{g(a-c)}+c_0\right] - V_2\sin^2\left[k_2\zeta/k_1\sqrt{g(a-c)}+c_0k_2/k_1\right], \end{aligned} \tag{17}$$

where A and B are two integration constants.

Generally, because of the unboundedness of $R_1^{''}$ in Eq.(16), the corrected solution (17) is unbounded as $\zeta\to\infty$. But by using the l'Hospital rule, we can prove that the first order perturbation solution will remain bounded, if and only if the condition[34]

$$I_\pm = \lim_{\zeta\to\pm\infty}\int_A^\zeta R_1^{'}(\zeta)V(\zeta)R_0(\zeta)\mathrm{d}\zeta = 0 \tag{18}$$

is satisfied. The condition in Eq.(18) implies a relationship between the system parameters and initial constants, which indicates the chaotic region in the parameter space. Under this condition, applying Eq.(14), Eq.(15) and l'Hospital rule, we obtain the superior and inferior limits of the corrected solution as

$$\begin{aligned} \overline{\lim_{x\to\pm\infty}} R_1 &\le \overline{\lim_{x\to\pm\infty}}\left[\frac{2}{\sqrt{g(a-c)}}V(\zeta)\frac{R_1^{'}R_0}{(R_1^{''-1})_\zeta}\right] + \overline{\lim_{x\to\pm\infty}}\left[-\frac{2}{\sqrt{g(a-c)}}V(\zeta)\frac{R_1^{''}R_0}{(R_1^{'-1})_\zeta}\right] \\ &= -\frac{3\sqrt{a}}{4g(a-c)}\underline{\lim_{x\to\pm\infty}} V(\zeta), \end{aligned} \tag{19}$$

$$\begin{aligned} \underline{\lim_{x\to\pm\infty}} R_1 &\ge \underline{\lim_{x\to\pm\infty}}\left[\frac{2}{\sqrt{g(a-c)}}V(\zeta)\frac{R_1^{'}R_0}{(R_1^{''-1})_\zeta}\right] + \underline{\lim_{x\to\pm\infty}}\left[-\frac{2}{\sqrt{g(a-c)}}V(\zeta)\frac{R_1^{''}R_0}{(R_1^{'-1})_\zeta}\right] \\ &= -\frac{3\sqrt{a}}{4g(a-c)}\overline{\lim_{x\to\pm\infty}} V(\zeta), \end{aligned} \tag{20}$$

which are correlated with that of $V(\zeta)$. We can derive the position ζ_0 from the zero-valued first derivative, i.e. $V_x(\zeta_0)=0$, then assert that $V(\zeta_0)$ is a minimum for the second derivative $V_{xx}(\zeta_0)>0$, or $V(\zeta_0)$ is a maximum for $V_{xx}(\zeta_0)<0$. Obviously, the values of k_1 and k_2 affect the largest and smallest values of $V(\zeta)$. If the values of k_1 and k_2 are given, the minimum and maximum $V(\zeta_0)$ will be fixed. For example, when $k_2/k_1=(4m+1)/2n$ (m and n are integers), the largest and smallest values of $V(\zeta)$ are V_1 and $-V_2$. Consequently, the superior and inferior limits of R_1 are $3V_2\sqrt{a}/4g(a-c)$ and $-3V_1\sqrt{a}/4g(a-c)$ respectively. On the other hand, from Eq.(17) we arrive at the spatial derivative of R_1 as

$$R_{1,\zeta} = \frac{2}{\sqrt{g(a-c)}}\left[R_{1,\zeta}^{''}\int_A^\zeta R_1^{'}V(\zeta)R_0\mathrm{d}\zeta - R_{1,\zeta}^{'}\int_B^\zeta R_1^{''}V(\zeta)R_0\mathrm{d}\zeta\right]. \tag{21}$$

Its superior and inferior limits read

$$\overline{\lim_{x\to\pm\infty}} R_{1,\zeta} \le \overline{\lim_{x\to\pm\infty}}\left[\frac{2}{\sqrt{g(a-c)}}V(\zeta)\frac{R_1^{'}R_0}{(R_{1,\zeta}^{''-1})_\zeta}\right] + \overline{\lim_{x\to\pm\infty}}\left[-\frac{2}{\sqrt{g(a-c)}}V(\zeta)\frac{R_1^{''}R_0}{(R_{1,\zeta}^{'-1})_\zeta}\right]$$

$$= -\frac{\sqrt{a}}{2g(a-c)} \varlimsup_{x\to\pm\infty} V(\zeta) + \frac{\sqrt{a}}{2g(a-c)} \varliminf_{x\to\pm\infty} V(\zeta), \tag{22}$$

$$\varlimsup_{x\to\pm\infty} R_{1,\zeta} \geq \varlimsup_{x\to\pm\infty} \left[\frac{2}{\sqrt{g(a-c)}} V(\zeta) \frac{R_1^{'} R_0}{(R_{1,\zeta}^{''-1})_\zeta}\right] + \varlimsup_{x\to\pm\infty} \left[-\frac{2}{\sqrt{g(a-c)}} V(\zeta) \frac{R_1^{''} R_0}{(R_{1,\zeta}^{'-1})_\zeta}\right]$$

$$= -\frac{\sqrt{a}}{2g(a-c)} \varliminf_{x\to\pm\infty} V(\zeta) + \frac{\sqrt{a}}{2g(a-c)} \varlimsup_{x\to\pm\infty} V(\zeta). \tag{23}$$

Here the superior and inferior limits of $R_{1,\zeta}$ are also determined by the superior and inferior limits of $V(\zeta)$. If the values of k_1 and k_2 are fixed, we can easily obtain the minimum and maximum of $V(\zeta)$ and the superior and inferior limits of $R_{1,\zeta}$. For example, when $k_2/k_1 = (4m+1)/2n$ (m and n are integers), the superior and inferior limits of $R_{1,\zeta}$ are $\sqrt{a}(V_1+V_2)/2g(a-c)$ and $-\sqrt{a}(V_1+V_2)/2g(a-c)$.

Now we choose the possible boundary conditions and physical parameters to explore the unpredictable chaotic orbit numerically. Here we take two laser wave lengths $\lambda_1 = 2\pi/k_1 = 850\text{nm}$, $\lambda_2 = 2\pi/k_2 = 850/3\text{nm}$ and s-wave scattering length $a_\text{s} = 5.5\,\text{nm}$ so that $g = 0.5$. We set parameters $\mu = 0.71215$, $\theta_x(x_0) = 0.0122$, $R_0(x_0) = 1.19338$, and $R_{0,x}(x_0) = 0$, which leads to $a = b = 1.42415$, $c = 0.0003$, $c_1 = 0.01$, $c_2 = 0.507$ from Eqs.(5), (9), (11) and (12). Taking the intensities of the weak lattice potentials as $V_1 = 0.01$ and $V_2 = 0.02$, and the integration constants as $c_0 = \pi$, $A = B = -\infty$, which are determined by values of the zeroth order solution and the first order correction respectively, we numerically plot the spatial evaluation of the first corrected solution from Eq.(17) as Fig.2(a). At points $x \approx -6$ and $x \approx 8$, the curve begins to become very dense and the system falls into the unpredictable chaotic motion region. In Fig.2(b), we show the spatial distribution of particle number density $\rho = (R_0 + R_1)^2$ with the same parameters as those in Fig.2(a), from which we can see the corresponding chaotic motion region of the particle number density.

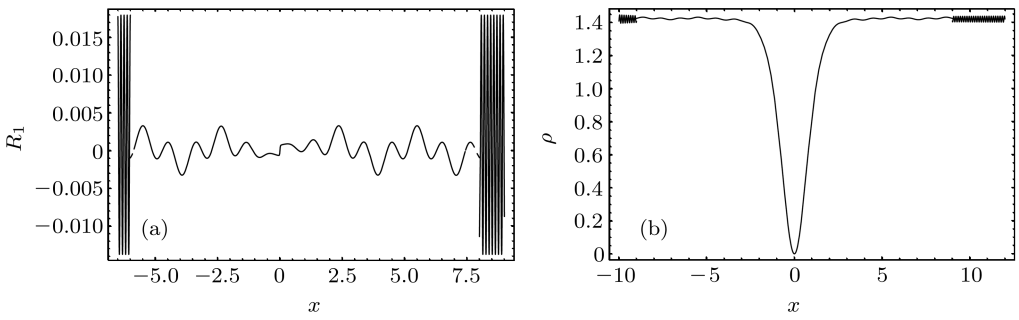


Fig.2. The spatial evolution of the first approximation R_1 (a) and the spatial distribution of the particle number density (b). The thick and black regions represent chaotic motion regions. The largest and smallest values of R_1 are limited by its superior and inferior limits. As in Fig.1, x, R_1 and ρ are dimensionless.

3. Generation and control of chaos

Chacón *et al* have investigated the Duffing-Holmes oscillator with two weak time-dependent periodic perturbations. They found that chaos can be suppressed by modulating the shape of a weak nonlinear periodic perturbation and a certain resonant frequency.[27,30] This hints broadly that if the time variable is replaced by the spatial coordinate, one also can suppress chaos by modulating the two weak spatially periodic potentials. The two weak spatially periodic potentials can be obtained experimentally by using two pairs of counter-propagating laser beams. Our work will illustrate the control of chaos by adjusting the laser wave vectors.

The boundedness condition of Eq.(18) in the preceding section contains the Melnikov chaos criterion,

$$M(\zeta_0) = I_+ - I_- = 2\int_{-\infty}^{\infty} R_1^{'} V(\zeta) R_0 \mathrm{d}\zeta = 0. \tag{24}$$

It is well known that the Melnikov function is proportional to the distance between the stable manifold and unstable manifold, and the simple zero Melnikov function means the intersection of the stable and unstable manifolds and indicates the existence of Smale-horseshoe chaos.[35] Under condition (24), Eq.(17) can be called the chaotic solution. Applying Eqs.(14) and (15) to Eq.(24), the zero Melnikov function results in the necessary condition promising the boundedness of solution (17),

$$\frac{\sin 2c_0}{\sin(2c_0k_2/k_1)} = \frac{k_2^2V_2\sinh(\pi/\sqrt{g(a-c)})}{k_1^2V_1\sinh(k_2\pi/k_1\sqrt{g(a-c)})} > 0. \tag{25}$$

Setting $Z = \sin 2c_0/\sin\left(\frac{2k_2}{k_1}c_0\right)$, when parameter Z satisfies $0 < Z \leq 1$, the chaotic region of parameter space reads

$$V_1 \geq \frac{k_2^2V_2\sinh(\pi/\sqrt{g(a-c)})}{k_1^2\sinh(k_2\pi/k_1\sqrt{g(a-c)})}. \tag{26}$$

In contrast, when parameter Z obeys $Z \geq 1$, chaotic region of parameter space becomes

$$V_1 \leq \frac{k_2^2V_2\sinh(\pi/\sqrt{g(a-c)})}{k_1^2\sinh(k_2\pi/k_1\sqrt{g(a-c)})}. \tag{27}$$

From inequalities (26) and (27) we can see that when the sign '=' is taken, they give the same boundary between the chaotic region and regular one in the parameter space. In inequality (26), the value region of V_1 above the boundary represents the chaotic region, and below the boundary is the regular region. However, in inequality (27), the value region of V_1 below the boundary is the chaotic region, and above the boundary represents the regular region.

To ensure that Eq.(25) is larger than zero, numerator $\sin 2c_0$ and denominator $\sin\frac{2k_2}{k_1}c_0$ should be positive or negative simultaneously. Consequently, constants $2c_0$ and $\frac{2k_2}{k_1}c_0$ should be in the first quadrant and second quadrant, where the values of sinusoidal function are positive, or in the third quadrant and fourth quadrant, where the values of sinusoidal function are negative. In order to conveniently compare the value of $\sin 2c_0$ with that of $\sin\frac{2k_2}{k_1}c_0$, we consider $2c_0$ and $\frac{2k_2}{k_1}c_0$ in the same quadrant simultaneously as the following two cases:

Case I $0 < Z \leq 1$, chaotic region of parameter space is determined by inequality (26). There are two subcases: (a) $k_2 < k_1$, $2c_0$, and $\frac{2k_2}{k_1}c_0$ are in the second quadrant simultaneously or the fourth quadrant simultaneously, i.e. $2c_0$, and $\frac{2k_2}{k_1}c_0 \in (2n\pi+\pi/2,\ 2n\pi+\pi)$ or $2c_0$, and $\frac{2k_2}{k_1}c_0 \in (2n\pi+3\pi/2,\ 2n\pi+2\pi)$ for an integer n; (b) $k_2 > k_1$, $2c_0$, and $\frac{2k_2}{k_1}c_0$ are in the first quadrant or the third quadrant, i.e. $2c_0$, and $\frac{2k_2}{k_1}c_0 \in (2n\pi,\ 2n\pi+\pi/2)$ or $2c_0$, and $\frac{2k_2}{k_1}c_0 \in (2n\pi+\pi,\ 2n\pi+3\pi/2)$.

Case II $Z \geq 1$, chaotic region of parameter space is determined by inequality (27). There are also two subcases: (a) $k_2 > k_1$, $2c_0$, and $\frac{2k_2}{k_1}c_0$ are in the second quadrant or the fourth quadrant, i.e. $2c_0$, and $\frac{2k_2}{k_1}c_0 \in (2n\pi+\pi/2,\ 2n\pi+\pi)$ or $2c_0$, and $\frac{2k_2}{k_1}c_0 \in (2n\pi+3\pi/2,\ 2n\pi+2\pi)$; (b) $k_2 < k_1$, $2c_0$, and $\frac{2k_2}{k_1}c_0$ are in the first quadrant or the third quadrant, i.e. $2c_0$, and $\frac{2k_2}{k_1}c_0 \in (2n\pi,\ 2n\pi+\pi/2)$ or $2c_0$, and $\frac{2k_2}{k_1}c_0 \in (2n\pi+\pi,\ 2n\pi+3\pi/2)$.

To ensure that $2c_0$ and $\frac{2k_2}{k_1}c_0$ are in the same quadrant simultaneously, the ratio between the two laser wave vectors must obey the relation $\frac{k_2}{k_1} \approx 1 \pm \frac{n\pi}{c_0}$, which is related to constant c_0. Combining Eq.(12) with Eq.(13), we know that integration constant $c_0 = x_0 \pm \frac{1}{\sqrt{g(a-c)}}Ar\mathrm{sech}\sqrt{\frac{a-\rho_0(x_0)}{a-c}}$ is correlated with the boundary conditions, so it cannot be exactly fixed in general. When boundary density $\rho_0(x_0)$ tends to homoclinic point a, constant c_0 approaches to infinity; otherwise, constant c_0 becomes relatively smaller. Although the value of c_0 is difficult to adjust exactly, we can take the simplest case where $n = 0$, i.e. $k_1 \approx k_2$, which makes it sure that $2c_0$ and $\frac{2k_2}{k_1}c_0$ both are in the same quadrant and have nothing to do with the value of c_0.

Comparing case I(a) with case II(a) we know that the chaotic region of the former is just the regular one of the latter, and the difference between the two cases comes from the change of the laser wave vectors only. Therefore, if constants $2c_0$ and $\frac{2k_2}{k_1}c_0$ are in the second or fourth quadrant and case I(a) corresponds to a chaotic state initially and we keep the approximation $k_1 \approx k_2$ and modulate the wave vectors from $k_2 < k_1$ to $k_2 > k_1$ experimentally, the system will transit from the chaotic state of case I(a) to the regular state of

case II(a), since the chaotic region and regular one are exchanged in such an operation. Of course, if case I(a) corresponds to a regular state, such a modulation will cause the transition from the regular state to the chaotic state. Obviously, if constants $2c_0$ and $\frac{2k_2}{k_1}c_0$ are in the first or third quadrant, namely case I(b) or case II(b), we can obtain a similar conclusion.

Under the condition $k_1 \approx k_2$ we are sure that $2c_0$ and $\frac{2k_2}{k_1}c_0$ are in the same quadrant, but do not know which quadrant they are in, since constant c_0 cannot be determined precisely. However, this does not affect the control of chaos. Experimentally, we can take a group of parameters V_1, V_2, g , a, c, k_1 and k_2 which satisfy the relations $k_1 \approx k_2$ and $k_2 < k_1$ to observe the structure of BEC initially. For example, Strekalov *et al*[36] have successfully detected the periodic structure of BEC by the Bragg scattering of an optical probe beam. In the observation, if BEC appears an aperiodic confuse distribution, we will consider it to be in a chaotic state initially, then according to the used parameters and applying Eq.(25), we can distinguish Z value of case I from that of case II. If the value of Z obeys $0 < Z \leq 1$ as in case I(a), we immediately deduce that the phases $2c_0$ and $\frac{2k_2}{k_1}c_0$ must be in the second or fourth quadrant. Fixing the other parameters and keeping relation $k_1 \approx k_2$, the quadrant of $2c_0$ and $\frac{2k_2}{k_1}c_0$ will be kept. In such a condition, we increase laser wave vector k_2 from $k_2 < k_1$ to $k_2 > k_1$, Z value will be changed from $0 < Z \leq 1$ of case I(a) to $Z \geq 1$ of case II(a). Such an operation will transit the initial chaotic state into the regular state. Of course, if the experimental parameters make the BEC be in the periodic regular region initially, we will observe the aperiodic chaotic structure after modulating the laser wave vectors from $k_2 < k_1$ to $k_2 > k_1$.

The chaotic region may be large or small, depending on integration constant c_0. For example, for $c_0 = 1$ from condition $2c_0$, and $\frac{2k_2}{k_1}c_0 \in (2n\pi+\pi/2,\ 2n\pi+\pi)$ we have the parameter region $k_2/k_1 \in (\pi/4, \pi/2)$ in which $2c_0$ and $\frac{2k_2}{k_1}c_0$ both are in the same (second) quadrant. If $c_0 = 2$ is set, the suitable parameter region will become $k_2/k_1 \in (\pi/4, 3\pi/8)$ in which $2c_0$ and $\frac{2k_2}{k_1}c_0$ are in the same (third) quadrant. Constant c_0 is decided by the boundary condition and can't be fixed exactly. However, whatever integration constant c_0 is, we can always modulate the laser wave vectors to $k_1 \approx k_2$ such that the system holds in the parameter region near $k_2/k_1 = 1$ as regions A and B in Fig.3. If the parameters satisfy relations $0 < Z \leq 1$ and $k_2 < k_1$, i.e. they fall into region A in Fig.3, the system will be in the chaotic state of case I(a) initially. Fixing V_1 and the other parameters, and increasing k_2 up to $k_2 \geq k_1$, the parameters enter region B and the system transits into the regular state of case II(a). In fact, from condition (25) we easily see that when critical value $k_2 = k_1$ is reached, this condition is no longer satisfied for $V_1 \neq V_2$, namely the necessary condition for onset of chaos cannot be realized in general. So the system leaves the chaotic state to enter the regular one. By using this method, we expect that the BEC system is controlled experimentally from the aperiodic chaotic state into the periodic regular structure.

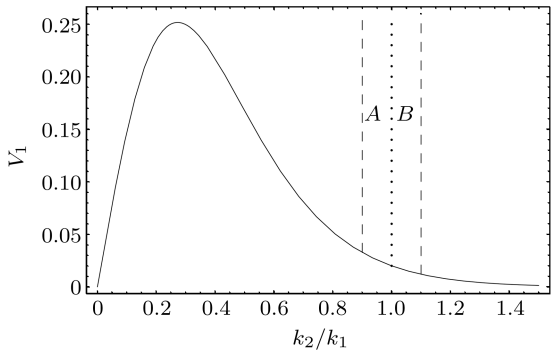


Fig.3. Schematic diagram of controlling chaos. The solid curve denotes the evolution of parameter V_1 with the ratio of k_2/k_1 from Eq.(25) for $Z = 1$, where $g = 0.5$, $a = 2$, $c = 1.6$, and $V_2 = 0.02$. If the parameters are taken in region A showing the system to be in chaotic state initially, the system will transit into a regular state by increasing laser wave vector k_2 to region B. Here V_1 is in units of two times the recoil energy.

We now try to explain the physical reason of the above conclusion. Taking potential $V(x) = V_1 \sin^2 k_1 x - V_2 \sin^2 k_2 x$ with $V_1 = 0.01$, $V_2 = 0.02$, $k_1 = 0.5$, and $k_2 = 0.4$, the spatial evolution of the potential is illustrated as the three same solid curves in Figs.4(a), 4(b) and 4(c). Keeping the other parameters invariable and increasing the value of wave vector k_2 up to 0.45, the potential function is plotted as the dashed line in Fig.4(a), where k_2 is always smaller than k_1. From Fig.4(a) we find that the period of dashed line becomes twice as large as that of the solid one and the number of the potential traps increases from 8 to 9 in the given spatial region in Fig.4. We continue to increase wave vector k_2 up to $k_2 = k_1 = 0.5$, the potential function is plotted as the dashed line in Fig.4(b). The number of the traps increases to 10, but the period of the potential function

suddenly fall down, it turns into simple harmonic oscillation in the form of sine or cosine wave. When k_2 is increased to 0.6, $k_2 > k_1$, the potential curve is as the dashed line in Fig.4(c). The period of the potential is the same as the solid line's and the number of the traps increases further to 14 in the given spatial region. From the profiles of the potential in Fig.4, we find that the number of the potential traps increases with the laser wave vector k_2, and speculate that the condensed atoms distribute anew in each trap. Once the well number exceeds a critical value, such a redistribution of atoms can lead to the transition between chaos and order.

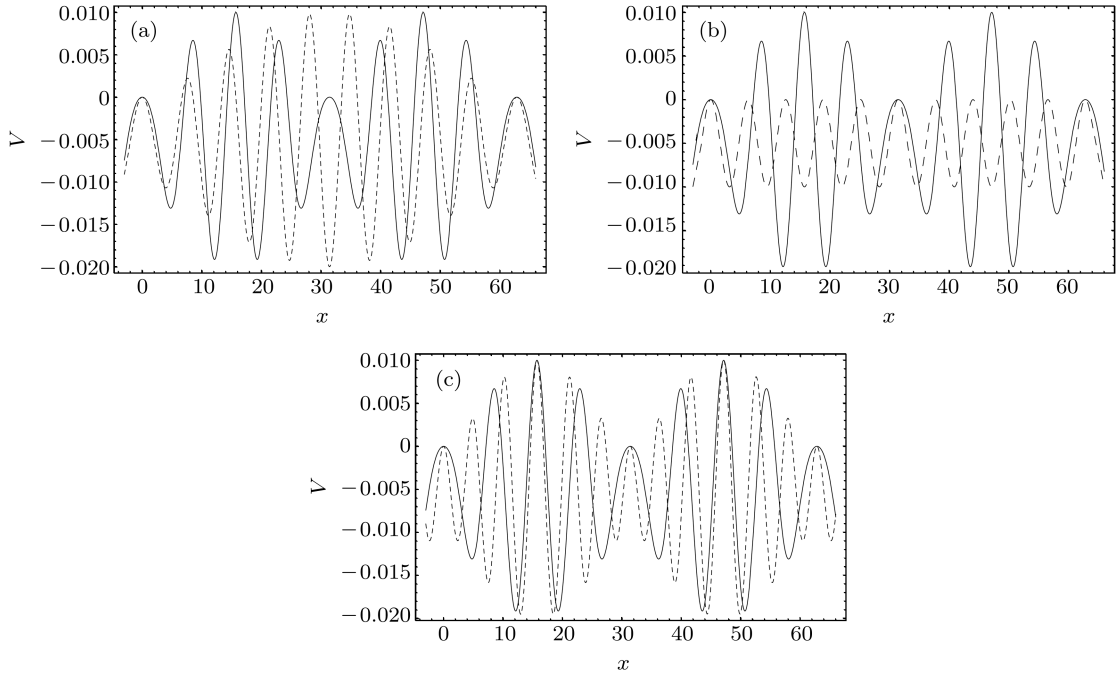


Fig.4. The profiles of the periodic potential function. The same solid curves in Fig.4(a), 4(b) and 4(c) are for parameters $V_1 = 0.01$, $V_2 = 0.02$, $k_1 = 0.5$, $k_2 = 0.4$. While after increasing wave vector k_2 and keeping the other parameters, potential $V(x)$ is plotted as the dashed curves for (a) $k_2 = 0.45$ ($k_2 < k_1$); (b) $k_2 = 0.5$ ($k_2 = k_1$); (c) $k_2 = 0.6$ ($k_2 > k_1$). Here dimensionless coordinate and potential strengths have been employed.

Now we discuss some details about the change of potential during adjusting the wave vector. It is certain that the changes of wave vector will lead to the displacements of some potential wells as in Figs.4 and 5. Similarly, Burger *et al* [3] have investigated the superfluid and dissipative dynamics of BEC in an optical lattice potential by making a displacement Δx of the magnetic trapping potential, which gives an impulse to the condensed atoms and results in an increase of speed. They find that the BEC regularly oscillates for a small displacements Δx, but when displacement Δx exceeds a critical value, the BEC loses its stability and the number of condensed particles decreases. From Fig.4 we can see that there are two most shallow wells in a spatial period. The stability of condensed atoms in the shallow wells could be lost more easily than that in the deeper wells, and the loss of stability may induce the transitions between chaotic state and regular one. We take the most shallow wells in Figs.4(b) and 4(c) to plot displacements Δx as in Fig.5. Figure 5(a) is a part of Fig.4(b) with $k_1 = k_2$ and from it we see that when one increases the value of the wave vector k_2, the site of the shallow trap displaces Δx from its original position. Here the displacement Δx is just the critical value, for $k_1 = k_2$ is a critical case. The BEC always oscillates regularly before k_2 value exceeds k_1 value. The displacement of the shoal trap becomes bigger and bigger with the increase of k_2. Figure 5(b) is a part of Fig.4(c) with $k_2 > k_1$. Comparing Fig.5(a) with Fig.5(b) we observe that the displacement in Fig.5(b) is bigger than the critical displacement in Fig.5(a). This will change the motion property of BEC. If the BEC is initially detected to be in an aperiodic chaotic state experimentally, in order to control chaos we must increase the value of k_2 up to $k_2 > k_1$ such that the periodic structure is observed.[36]

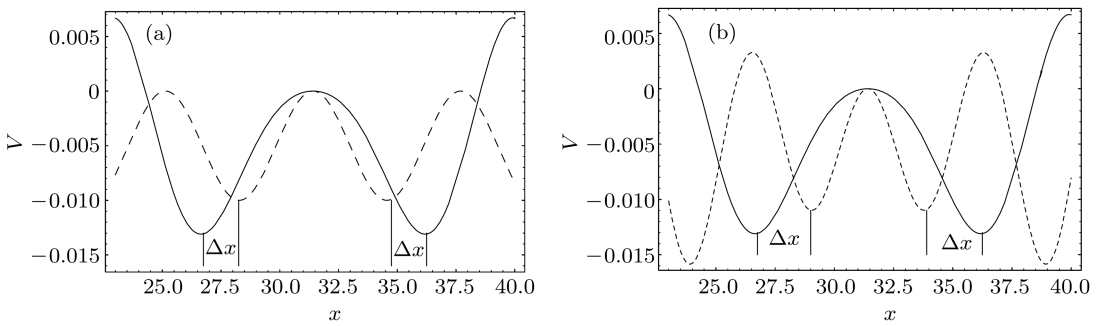


Fig.5. Schematic diagram of the spatial displacement for the most shallow wells. (a) A part of Fig.4(b), where the solid curve corresponds to $k_2 = 0.4 < k_1$ and dashed curve to $k_2 = 0.5 = k_1$. Displacement Δx of the trap site is shown as a critical value here. (b) A part of Fig.4(c), where the solid curve is the same as that in Fig.5(a) and dashed curve corresponds to $k_2 = 0.6 > k_1$. Displacement Δx has increased to a value that exceeds the critical value in Fig.5(a).

4. Conclusions and discussion

In this paper the investigated system is a BEC trapped in the supplemental potential consisting of two laser standing waves and described by the 1D stationary state GPE. We consider the laser intensities to be so weak that they can be treated as a perturbation, the zeroth order homoclinic solution of the GPE and its first order correction are constructed by applying direct perturbation expansion method. Applying the Melnikov chaos criterion, we find the corrected solution to be a chaotic solution and obtain the superior and inferior limits of the motion region in which the macroscopic quantum state is unpredictable. The numerical simulation method is also used to solve the unperturbed GPE, and a chaotic attractor is shown in the equivalent phase space. The spatial evolutions of the first order corrected solution and particle number density are also potted numerically, just as we theoretically expect the spatial chaos existence in the images. Adopting the Melnikov-function technique, we obtain the chaotic region parameter space, which is correlated with constant c_0 determined by boundary position x_0 and particle number density $\rho_0(x_0)$. Because of chaos sensitively depending on the boundary condition, and the boundary condition is very difficult to fix exactly, we restrict ourselves to a simple case, where the existence of chaotic region is independent of boundary constant c_0. It is shown that if one keeps k_1 being a constant and makes k_2 cross a critical value, the chaotic region can be transformed into regular one or the other way round. So we can transform the aperiodic chaotic state into the periodic regular state or the other way round by modulating the laser wave vector.

We also illustrate numerically that the modulation to the laser wave vectors leads to the changes of the number and site of potential wells. The change of well number implies that the condensed particles are redistributed into each well, and the change of well site means that the i-th potential well displaces a distance Δx_i, which gives an impulse to the condensed atoms in the well. When the change of well number and the displacement of well site exceed the corresponding critical values, the motion property of the condensate is varied between chaotic state and periodic one.

It is worth noting the feasibility of experimental observation on the generation and control of chaos. The process of the experimental operation contains the determination of initial states and the adjustments to the laser wave vector. By the Bragg scattering of an optical probe beam,[36] we can detect the periodic structure or aperiodic chaotic state of the BEC initially. And then we keep the approximation $k_2 \approx k_1$ and adjust k_2 from $k_2 < k_1$ to $k_2 \geq k_1$, the initial chaos is controlled or the initial periodic structure is destroyed and chaos is formed. Our results have provided a feasible scheme for creating and controlling chaos. Therefore, we expect our scheme to be experimentally realized in the near future.

References

[1] Leggett A J 2001 *Rev. Mod. Phys.* **73** 307
Aderson B P and Kasevich M A 1998 *Science* **282** 1686
Wu Y, Yang X and Xiao Y 2001 *Phys. Rev. Lett.* **86** 2200
Liu W M, Wu B and Niu Q 2000 *Phys. Rev. Lett.* **84** 2294

[2] Hu Z, Du C and Li S 2003 *Chin. Phys.* **12** 708
Xu Z, Zhou S, Qu Q, Liu H, Zhou S and Wang Y 2006 *Acta. Phys. Sin.* **55** 5643 (in Chinese)
Xie B and Jing H 2002 *Chin. Phys.* **11** 115

[3] Burger S, Cataliotti F S, Fort C, Minardi F, Inguscio M, Chiofalo M L and Tosi M P 2001 *Phys. Rev. Lett.* **86** 4447

[4] Wu B and Niu Q 2001 *Phys. Rev.* A **64** 061603R

[5] Smerzi A, Fantoni S, Giovanazzi S and Shenoy S R 1997 *Phys. Rev. Lett.* **79** 4950

[6] Wang G, Fu L, Zhao H and Liu J 2005 *Acta Phys. Sin.* **54** 5003 (in Chinese)

[7] Drummond P D, Kheruntsyan K V and He H 1998 *Phys. Rev. Lett.* **81** 3055
Mahmud K W, Perry H and Reinhardt W P 2005 *Phys. Rev.* A **71** 023615

[8] Liang Z X, Zhang Z D and Liu W M 2005 *Phys. Rev. Lett.* **94** 050402
Huang G 2004 *Chin. Phys.* **13** 1866

[9] Liu J, Zhang C, Raizen Mark G and Niu Q 2006 *Phys. Rev.* A **73** 013601

[10] Chong G, Hai W and Xie Q 2004 *Phys. Rev.* E **70** 036213

[11] Chong G, Hai W and Xie Q 2004 *Chaos* **14** 217
Chong G, Hai W and Xie Q 2005 *Phys. Rev.* E **71** 016202

[12] Saito H and Ueda M 2001 *Phys. Rev. Lett.* **86** 1406

[13] Filho V S, Gammal A, Frederico T and Tomio L 2000 *Phys. Rev.* A **62** 033605

[14] Coullet P and Vandenberghe N 2001 *Phys. Rev.* E **64** 025202

[15] Thommen Q, Garreau J C and Zehnlé V 2003 *Phys. Rev. Lett.* **91** 210405

[16] Zhang C, Liu J, Raizen M G and Niu Q 2004 *Phys. Rev. Lett.* **93** 074101

[17] Elyutin P V 2001 *Phys. Rev.* E **64** 016607

[18] Abdullaev F Kh and Kraenke R A 2000 *Phys. Rev.* A **62** 023613

[19] Xie Q and Hai W 2005 *Eur. Phys. J.* D **33** 265
Cheng R and Liang J Q 2007 *Chin. Phys.* **16** 834

[20] Hai W, Lee C, Chong G and Shi L 2002 *Phys. Rev.* E **66** 026202
Lee C, Hai W, Shi L, Zhu X and Gao K 2001 *Phys. Rev.* A **64** 053604

[21] Ott E, Grebogi C and Yorke J A 1990 *Phys. Rev. Lett.* **64** 1196
Ott E, Grebogi C and Yorke J A 1990 *Phys. Rev. Lett.* **64** 2837
Yue L J and Shen K 2005 *Chin. Phys.* **14** 60
Bai L, Zhang R, Weng J Q, Luo X S and Fang J Q 2006 *Chin. Phys.* **15** 1226
Zheng Y A 2006 *Chin. Phys.* **15** 2549

[22] Dressler U and Nitsche G 1992 *Phys. Rev. Lett.* **68** 1
Huang W, Yu C X, Zheng J, Xie J L, Liu W D, Feng D L and Ding W X 2004 *Chin. Phys.* **13** 1913
Yu H J 2005 *Acta Phys. Sin.* **54** 5053 (in Chinese)

[23] Buchner T and Żebrowski J J 2001 *Phys. Rev.* E **63** 016210
Dykstra R, Tang D Y and Heckenberg N R 1998 *Phys. Rev.* E **57** 6596
Yamasue K and Hikihara T 2006 *Phys. Rev.* E **73** 036209

[24] Konishi K, Kokame H and Hirata K 2000 *Phys. Rev.* E **62** 384

[25] Beck O, Amann A, Schöll E, Socolar J E S and Just W 2002 *Phys. Rev.* E **66** 016213
Tziperman E, Scher H, Zebiak S E and Cane M A 1997 *Phys. Rev. Lett.* **79** 1034

[26] Kushibe M, Liu Y and Ohtsubo J 1996 *Phys. Rev.* E **53** 4502

[27] Chacón R 1995 *Phys. Rev.* E **51** 761
Chacón R and Díaz Bejarano J 1993 *Phys. Rev. Lett.* **71** 3103
Meucci R, Gadomski W, Ciofini M and Arecchi F T 1994 *Phys. Rev.* E **49** R2528
Chen L and Wang D S 2007 *Acta Phys. Sin.* **56** 91 (in Chinese)

[28] Liu W M, Fan W B, Zheng W M, Liang J Q and Chui S T 2002 *Phys. Rev. Lett.* **88** 170408
Damski B, Zakrzewski J, Santos L, Zoller P and Lewenstein M 2003 *Phys. Rev. Lett.* **91** 080403

[29] Cohen J L, Dubetsky B and Berman P R 1999 *Phys. Rev.* A **60** 3982

[30] Xia B and Hai W 2005 *Chin. Opt. Lett.* **3** 373

[31] Diener R B, Georgakis G A, Zhong J, Raizen M and Niu Q 2001 *Phys. Rev.* A **64** 033416

[32] Jackson A D, Kavoulakis G M and Pethick C J 1998 *Phys. Rev.* A **58** 2417

[33] Hai W, Xie Q and Fang J 2005 *Phys. Rev.* A **72** 012116

[34] Hai W, Feng M, Zhu X, Shi L, Gao K and Fang X 2000 *Phys. Rev.* A **61** 052105

[35] Liu Z 1994 *Perturbation Criteria for Chaos* (Shanghai: Shanghai Scientific and Technological Education Press) (in Chinese)

[36] Strekalov D V, Turlapov A, Kumarakrishnan A and Sleator T 2002 *Phys. Rev.* A **66** 023601